Appl. Math. Mech. -Engl. Ed., **35**(11), 1387–1400 (2014)
DOI 10.1007/s10483-014-1870-7

Applied Mathematics and Mechanics (English Edition)

Differential transformation method for studying flow and heat transfer due to stretching sheet embedded in porous medium with variable thickness, variable thermal conductivity, and thermal radiation*

M. M. KHADER[1,2], A. M. MEGAHED[2]

(1. Department of Mathematics and Statistics, College of Science, Al-Imam Mohammad Ibn Saud Islamic University (IMSIU), Riyadh 11432, Saudi Arabia;
2. Department of Mathematics, Faculty of Science, Benha University, Benha 13518, Egypt)

Abstract This article presents a numerical solution for the flow of a Newtonian fluid over an impermeable stretching sheet embedded in a porous medium with the power law surface velocity and variable thickness in the presence of thermal radiation. The flow is caused by non-linear stretching of a sheet. Thermal conductivity of the fluid is assumed to vary linearly with temperature. The governing partial differential equations (PDEs) are transformed into a system of coupled non-linear ordinary differential equations (ODEs) with appropriate boundary conditions for various physical parameters. The remaining system of ODEs is solved numerically using a differential transformation method (DTM). The effects of the porous parameter, the wall thickness parameter, the radiation parameter, the thermal conductivity parameter, and the Prandtl number on the flow and temperature profiles are presented. Moreover, the local skin-friction and the Nusselt numbers are presented. Comparison of the obtained numerical results is made with previously published results in some special cases, with good agreement. The results obtained in this paper confirm the idea that DTM is a powerful mathematical tool and can be applied to a large class of linear and non-linear problems in different fields of science and engineering.

Key words Newtonian fluid, stretching sheet, differential transformation method (DTM), thermal radiation, variable thermal conductivity, variable thickness

Chinese Library Classification O362
2010 Mathematics Subject Classification 76D05

Nomenclature

A, b,	constants;	k_0,	permeability parameter;
$C_{\rm f}$,	skin friction coefficient;	m,	velocity power index;
c_p,	specific heat at constant pressure;	Nu,	Nusselt number;
D,	porous parameter;	Pr,	Prandtl number;
$f(\eta)$,	similarity variable;	$q_{\rm r}$,	radiative heat flux;
k,	permeability of porous medium;	$q_{\rm eff}$,	effective conduction-radiation flux;
k^*,	mean absorption coefficient;	R,	radiation parameter;

* Received Jun. 12, 2013 / Revised Feb. 19, 2014
Corresponding author M. M. KHADER, Professor, E-mail: mohamedmbd@yahoo.com

Re_x, local Reynolds number;
T, temperature of fluid;
T_w, temperature of sheet;
T_∞, free-stream temperature;
u, velocity component in x-direction;
v, velocity component in y-direction;
U, stretching velocity;
U_0, reference velocity;
v_w, suction or injection velocity;
x, coordinate measured along surface;
y, coordinate normal to surface.

Greek symbols

α, thickness of wall parameter;
η, similarity variable;
ϵ, thermal conductivity parameter;
κ, fluid thermal conductivity;
κ_{eff}, effective thermal conductivity;
ψ, stream velocity function;
ρ, fluid density;
σ^*, Stefan-Boltzmann constant;
θ, dimensionless temperature;
μ, fluid viscosity;
ν, kinematic viscosity of the fluid.

Subscripts

∞, free stream condition;
w, condition at surface.

1 Introduction

The study of flow and heat transfer of a Newtonian fluid over a stretching surface issuing from slit has gained considerable attention of many researchers due to its importance in many industrial applications, such as extraction of polymer sheet, wire drawing, paper production, glass-fiber production, hot rolling, solidification of liquid crystals, petroleum production, continuous cooling and fibers spinning, and exotic lubricants and suspension solutions. Much work on the boundary-layer Newtonian fluids has been carried out both experimentally and theoretically. Crane[1] was the first one who studied the stretching problem taking into account the fluid flow over a linearly stretched surface. There has been a great deal of the work done on Newtonian fluid flow and heat transfer over a stretching surface, but only a few recent studies are cited here. Gupta and Gupta[2] analyzed the stretching problem with a constant surface temperature, while Soundalgekar and Ramana[3] investigated the constant surface velocity case with a power-law temperature variation. Grubka and Bobba[4] have analyzed the stretching problem for a surface moving with a linear velocity and with a variable surface temperature. Chen and Char[5] investigated the heat transfer characteristics over a continuous stretching sheet with variable surface temperature. Using the homotopy analysis method (HAM), series solutions were obtained by Hayat et al.[6] for the stretching sheet problem with mixed convection.

Despite the practical importance of the flow in a porous medium, all the above-mentioned works do not however consider the situations where the flow in fluid-saturated porous media arises. The study of the flow in fluid-saturated porous media due to a stretching sheet is important in engineering problems, such as the design of building components for energy consideration, soil science, mechanical engineering, control of pollutant spread in groundwater, thermal insulation systems, compact heat exchangers, solar power collectors, and food industries. Because of such important practical applications, many investigators have modeled the behavior of a boundary layer flow embedded in a porous medium. Then, extensive studies were conducted by many researchers[7–10]. In all the previous investigations, the effects of radiation on the flow and heat transfer have not been provided. Radiative heat transfer flow is very important in manufacturing industries for the design of reliable equipments, nuclear plants, gas turbines, and various propulsion devices for aircraft, missiles, satellites, and space vehicles. Also, the effects of thermal radiation on the forced and free convection flows are important in the context of space technology and processes involving high temperature. Based on these applications, Hossain et al.[11–12] and Elbashbeshy and Demain[13] studied the thermal radiation of a gray fluid which is emitting and absorbing radiation in non-scattering medium. Abel and Mahesha[14] studied the effect of radiation in different situations. Recently, Battaler[15] studied

the effect of thermal radiation on the laminar boundary layer about a flat plate. Historically, the study on boundary layer flows over a stretching sheet with variable thickness was studied by Fang et al.[16]. However, so far no attention has been given to the effects of the non-flatness on the stretching sheet problems considering a variable sheet thickness. The purpose of the present paper is to investigate the numerical solution for the variable thermal conductivity effect on the flow and heat transfer of a Newtonian fluid-saturated porous medium over a stretching sheet with variable thickness in the presence of thermal radiation.

Most non-linear differential equations do not have exact solutions, so approximate and numerical techniques[17–22] must be used. The differential transformation method (DTM) is a semi-numerical-analytic-technique that formalizes the Taylor series in a totally different manner. It was first introduced by Zhou in a study about electrical circuits[23]. Borhanifar and Abazari[24–25] used it for solving of the linear and non-linear problems. In this paper, we extended DTM for applying to the search for the numerical solutions of the introduced problem. The DTM plays an important rule in recent researches in this field. It has been shown that this procedure is a powerful tool for solving various kinds of problems[26–30]. This technique reduces the problem to a system of algebraic equations. In this work, we will use the Newton iteration method to solve the resulting system of algebraic equations.

2 Formulation of problem

Consider a steady, two-dimensional boundary layer flow of an incompressible Newtonian fluid over a continuously impermeable stretching sheet embedded in a porous medium. The origin is located at a slit, through which the sheet (see Fig. 1) is drawn through the fluid medium. The x-axis is chosen along the sheet and y-axis is taken normal to it. The stretching surface has the velocity $U_{\mathrm{w}} = U_0(x+b)^m$, where U_0 is the reference velocity. We assume that the sheet is not flat in which it is specified as $y = A(x+b)^{\frac{1-m}{2}}$, where A is a very small constant so that the sheet is sufficiently thin and m is the velocity power index. We must observe that our problem is valid only for $m \neq 1$, because for $m = 1$, the problem reduces to a flat sheet. Likewise, the fluid properties are assumed to be constant except for thermal conductivity variations in the temperature. Making the usual boundary layer approximations for the Newtonian fluid, the steady two-dimensional boundary-layer equations taking into account the thermal radiation effect in the energy equation can be written as

$$\frac{\partial u}{\partial x} + \frac{\partial v}{\partial y} = 0, \tag{1}$$

$$u\frac{\partial u}{\partial x} + v\frac{\partial u}{\partial y} = \nu\frac{\partial^2 u}{\partial y^2} - \frac{\mu}{\rho k}u, \tag{2}$$

$$\rho c_p\Big(u\frac{\partial T}{\partial x} + v\frac{\partial T}{\partial y}\Big) = \frac{\partial}{\partial y}\Big(\kappa\frac{\partial T}{\partial y}\Big) - \frac{\partial q_{\mathrm{r}}}{\partial y}, \tag{3}$$

where u and v are the velocity components in x- and y-directions, respectively. ρ and κ are the fluid density and the thermal conductivity, respectively. T is the temperature of the fluid, ν is the fluid kinematic viscosity, c_p is the specific heat at constant pressure, μ is the fluid viscosity, k is the permeability of the porous medium, and q_{r} is the radiative heat flux. The radiative heat flux q_{r} is employed according to Rosseland approximation[31] such that

$$q_{\mathrm{r}} = -\frac{4\sigma^*}{3k^*}\frac{\partial T^4}{\partial y}, \tag{4}$$

where σ^* is the Stefan-Boltzmann constant, and k^* is the mean absorption coefficient. Following Raptis[23], we assume that the temperature differences within the flow are sufficiently small such

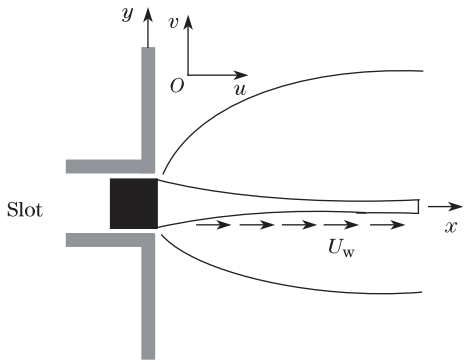

Fig. 1 Schematic of stretching sheet with variable sheet thickness

that T^4 may be expressed as a linear function of the temperature. Expanding T^4 in a Taylor series about T_∞ and neglecting higher-order terms, we have

$$T^4 \cong 4T_\infty^3 T - 3T_\infty^4. \tag{5}$$

The physical and mathematical advantage of the Rosseland formula (5) consists of the fact that it can be combined with Fourier's second law of conduction to an effective conduction-radiation flux q_{eff} in the form

$$q_{\text{eff}} = -\Big(\kappa + \frac{16\sigma^* T_\infty^3}{3k^*}\Big)\frac{\partial T}{\partial y} = -\kappa_{\text{eff}}\frac{\partial T}{\partial y}, \tag{6}$$

where $\kappa_{\text{eff}} = \kappa + \frac{16\sigma^* T_\infty^3}{3k^*}$ is the effective thermal conductivity. Thus, the steady energy balance equation including the net contribution of the radiation emitted from the hot wall and absorbed in the colder fluid, takes the form

$$\rho c_p\Big(u\frac{\partial T}{\partial x} + v\frac{\partial T}{\partial y}\Big) = \frac{\partial}{\partial y}\Big(\kappa_{\text{eff}}\frac{\partial T}{\partial y}\Big). \tag{7}$$

To obtain the similarity solutions, it is assumed that the permeability of the porous medium $k(x)$ is of the form

$$k(x) = k_0(x+b)^{1-m}, \tag{8}$$

where k_0 is the permeability parameter. The boundary conditions can be written as

$$u\Big(x, A(x+b)^{\frac{1-m}{2}}\Big) = U_0(x+b)^m, \quad v\Big(x, A(x+b)^{\frac{1-m}{2}}\Big) = 0, \quad T\Big(x, A(x+b)^{\frac{1-m}{2}}\Big) = T_{\text{w}}, \tag{9}$$

$$u(x,\infty) = 0, \qquad T(x,\infty) = T_\infty. \tag{10}$$

The mathematical analysis of the problem is simplified by introducing the following dimensionless coordinates:

$$\begin{cases} \zeta = y\sqrt{U_0(\frac{m+1}{2})\Big(\frac{(x+b)^{m-1}}{\nu}\Big)}, \quad \psi(x,y) = \sqrt{\nu U_0(\frac{2}{m+1})(x+b)^{m+1}}F(\zeta), \\ \Theta(\zeta) = \Big(\frac{T-T_\infty}{T_{\text{w}}-T_\infty}\Big), \end{cases} \tag{11}$$

where ζ is the similarity variable, $\psi(x,y)$ is the stream function which is defined in the classical form as $u = \frac{\partial\psi}{\partial y}$ and $v = \frac{-\partial\psi}{\partial x}$, and $\Theta(\zeta)$ is the dimensionless temperature.

In this study, the equation for the dimensionless thermal conductivity κ is generalized for the temperature dependence as follows[33–34]:

$$\kappa = \kappa_\infty(1+\epsilon\Theta), \tag{12}$$

where κ_∞ is the ambient thermal conductivity, and ϵ is the thermal conductivity parameter.

Upon using these variables, the boundary layer governing equations (1)−(3) can be written in the following non-dimensional form:

$$F''' + FF'' - \frac{2m}{m+1}F'^2 - DF' = 0, \tag{13}$$

$$\Big(\frac{1+R}{Pr}\Big)\Big((1+\epsilon\Theta)\theta'' + \epsilon\Theta'^2\Big) + F\Theta' = 0, \tag{14}$$

where $D = \frac{2\nu}{k_0U_0(m+1)}$ is the porous parameter, $Pr = \frac{\mu c_p}{\kappa_\infty}$ is the Prandtl number, and $R = \frac{16\sigma^*T_\infty^3}{3k^*\kappa_\infty}$ is the radiation parameter. The transformed boundary conditions are

$$F(\alpha) = \alpha\Big(\frac{1-m}{1+m}\Big), \quad F'(\alpha) = 1, \quad \Theta(\alpha) = 1, \tag{15}$$

$$F'(\infty) = 0, \quad \Theta(\infty) = 0, \tag{16}$$

where $\alpha = A\sqrt{\frac{U_0(m+1)}{2\nu}}$ is a parameter related to the thickness of the wall, and $\eta = \alpha = A\sqrt{\frac{U_0(m+1)}{2\nu}}$ indicates the plate surface. In order to facilitate the computation, we define $F(\zeta) = F(\eta-\alpha) = f(\eta)$ and $\Theta(\zeta) = \Theta(\eta-\alpha) = \theta(\eta)$. The similarity equations and the associated boundary conditions become

$$f''' + ff'' - \frac{2m}{m+1}f'^2 - Df' = 0, \tag{17}$$

$$\Big(\frac{1+R}{Pr}\Big)((1+\epsilon\theta)\theta'' + \epsilon\theta'^2) + f\theta' = 0, \tag{18}$$

$$f(0) = \alpha\Big(\frac{1-m}{1+m}\Big), \quad f'(0) = 1, \quad \theta(0) = 1, \tag{19}$$

$$f'(\infty) = 0, \quad \theta(\infty) = 0, \tag{20}$$

where the prime denotes differentiation with respect to η. Based on the variable transformation, the solution domain will be fixed from 0 to ∞. The physical quantities of primary interest are the local skin-friction coefficient C_f and the local Nusselt number Nu, which are defined as

$$C_\mathrm{f} = -2\sqrt{\frac{m+1}{2}}Re_x^{\frac{-1}{2}}f''(0), \quad Nu = -\sqrt{\frac{m+1}{2}}Re_x^{\frac{1}{2}}\theta'(0), \tag{21}$$

where $Re_x = \frac{U_\mathrm{w}X}{\nu}$ is the local Reynolds number, and $X = x + b$.

3 Basic definitions of DTM

In the DTM, the given differential equation and related initial conditions are transformed into a recurrence equation that finally leads to the solution of a system of algebraic equations as coefficients of a power series solution. This method is useful for obtaining exact and approximate solutions of linear and nonlinear differential equations. There is no need for linearization or

perturbations, and large computational work and round-off errors are avoided. It has been used to solve a large class of linear and nonlinear differential equations with approximations effectively, easily, and accurately.

The basic definitions of DTM are introduced as follows. With reference to the articles[26,28], we introduce in this section the basic definitions of the one-dimensional DTM.

Definition 1 *If $f(\eta)$ is an analytic function in the domain $\Omega = [0, T]$, then it will be differentiated continuously with respect to time η,*

$$\frac{\mathrm{d}^k f(\eta)}{\mathrm{d}\eta^k} = \phi(\eta, k), \quad \forall\, \eta \in \Omega. \tag{22}$$

For any point $\eta = \eta_i$ in $[0, T]$, we have $\phi(\eta, k) = \phi(\eta_i, k)$, where k belongs to the set of non-negative integers $\mathbb{N}_0$. Therefore, (22) can be written as

$$F(k) = \phi(\eta_i, k) = \Big(\frac{\mathrm{d}^k f(\eta)}{\mathrm{d}\eta^k}\Big)_{\eta=\eta_i}, \quad \forall\, k \in \mathbb{N}_0, \tag{23}$$

where $F(k) \in \mathbb{R}^{n\times n}$ is called the spectrum of $f(\eta)$ at $\eta = \eta_i$ in the domain $\mathbb{N}_0$. Also, $F(k)$ is called the differential transform of the function $f(\eta)$.

Definition 2 *If $f(\eta)$ can be expressed by Taylor's series about the fixed point η_i, then $f(\eta)$ can be represented as*

$$f(\eta) = \sum_{k=0}^{\infty} \frac{f^{(k)}(\eta_i)}{k!}(\eta - \eta_i)^k. \tag{24}$$

If $f_n(\eta)$ is the n-partial sums of Taylor's series (24), then

$$f_n(\eta) = \sum_{k=0}^{n} \frac{f^{(k)}(\eta_i)}{k!}(\eta - \eta_i)^k + R_{n+1}(\eta), \tag{25}$$

where $f_n(\eta)$ is called the nth Taylor polynomial for $f(\eta)$ about η_i, and $R_{n+1}(\eta)$ is the remainder term. Now, using (23), (24) reduces to

$$f(\eta) = \sum_{k=0}^{\infty} F(k)(\eta - \eta_i)^k, \tag{26}$$

and the n-partial sum of Taylor's series (25) reduces to

$$f_n(\eta) = \sum_{k=0}^{n} F(k)(\eta - \eta_i)^k + R_{n+1}(\eta). \tag{27}$$

For simplicity, we assume the particular case $\eta_i = 0$ (Maclaurin). Then, (26) reduces to

$$f(\eta) = \sum_{k=0}^{n} F(k)\eta^k + R_{n+1}(\eta). \tag{28}$$

It is clear that the concept of differential transformation is based upon the Taylor series expansion. The values of function $F(k)$ at values of argument k are referred to as discrete, i.e., $F(0)$ is known as the zero discrete, $F(1)$ as the first discrete, etc. The more discrete available, the more precise it is possible to restore the unknown function. The function $f(\eta)$ consists of the transformed function $F(k)$, and its value is given by the sum of the transformed function with η^k as its coefficient. In real applications, at the larger values of argument k, the discrete of spectrum reduces rapidly.

From the above definitions, it can be found that the concept of the one-dimensional differential transform is derived from the Taylor series expansion. With (23) and (26), the fundamental mathematical operations performed by one-dimensional differential transform can readily be obtained and listed in Table 1.

Table 1 Fundamental operations of one-dimension DTM

Original function	Transformed function
$w(\eta) = u(\eta) \pm v(\eta)$	$W(k) = U(k) \pm V(k)$
$w(\eta) = c\,u(\eta)$	$W(k) = c\,U(k)$
$w(\eta) = \frac{\mathrm{d}}{\mathrm{d}\eta}u(\eta)$	$W(k) = (k+1)U(k+1)$
$w(\eta) = \frac{\mathrm{d}^2}{\mathrm{d}\eta^2}u(\eta)$	$W(k) = (k+1)(k+2)U(k+2)$
$w(\eta) = \frac{\mathrm{d}^m}{\mathrm{d}\eta^m}u(\eta)$	$W(k) = (k+1)\cdots(k+m)U(k+m)$
$w(\eta) = u(\eta)v(\eta)$	$W(k) = U(k) \otimes V(k) = \sum_{l=0}^{k} U(l)V(l-k)$

4 Solution procedure using DTM

Our aim in this paper is to use the DTM to solve numerically (17)–(18) at the bounded domain $(0, \eta_\infty)$ with the boundary conditions (19)−(20). Using the DTM on (17)−(18), and from Table 1, we get

$$\begin{aligned}
&(k+1)(k+2)(k+3)F(k+3)\\
&= -\sum_{r=0}^{k}(k-r+1)(k-r+2)F(r)F(k-r+2)\\
&\quad + \Big(\frac{2m}{m+1}\Big)\sum_{r=0}^{k}(r+1)(k-r+1)F(r+1)F(k-r+1) + D(k+1)F(k+1), \qquad (29)
\end{aligned}$$

$$\begin{aligned}
&(k+1)(k+2)\Theta(k+2)\\
&= \sum_{r=0}^{k} -\epsilon(k-r+1)(k-r+2)\Theta(r)\Theta(k-r+2)\\
&\quad - \epsilon(r+1)(k-r+1)\Theta(r+1)\Theta(k-r+1)\\
&\quad - \Big(\frac{Pr}{1+R}\Big)(k-r+1)F(r)\Theta(k-r+1), \qquad (30)
\end{aligned}$$

where $F(k)$ and $\Theta(k)$ are the differential transforms of $f(\eta)$ and $\theta(\eta)$, respectively.

We choose suitable initial conditions

$$F(0) = \alpha\Big(\frac{1-m}{1+m}\Big), \qquad F(1) = \frac{1}{2}, \qquad F(2) = \frac{1}{6}c_0, \qquad \Theta(0) = 1, \qquad \Theta(1) = \frac{1}{2}c_1 \qquad (31)$$

for arbitrary constants c_0 and c_1. From (29)−(30), for $k = 0, 1, \cdots$, and using (31), we get

$$\begin{cases} F(3) = \dfrac{1}{6}\Big(-2F(0)F(2) + \Big(\dfrac{2m}{m+1}\Big)(F(1))^2 + DF(1)\Big) \\ \qquad = \dfrac{1}{6}\Big(-\dfrac{1}{3}\alpha c_0\Big(\dfrac{1-m}{1+m}\Big) + \dfrac{0.5m}{m+1} + 0.5D\Big), \\ \Theta(2) = \dfrac{1}{2}\Big(-2\epsilon\Theta(0)\Theta(2) - \epsilon(\Theta(1))^2 - \Big(\dfrac{Pr}{1+R}\Big)F(0)\Theta(1)\Big) \\ \qquad = \dfrac{1}{2}\Big(-2\epsilon\Theta(2) - 0.25\epsilon\, c_1^2 - \Big(\dfrac{0.5\alpha c_1 Pr}{1+R}\Big)\Big(\dfrac{1-m}{1+m}\Big)\Big), \\ F(4) = \dfrac{1}{24}\Big(-6F(0)F(3) - 2F(1)F(2) + \Big(\dfrac{8m}{1+m}\Big)F(1)F(2) + 2DF(2)\Big) \\ \qquad = \dfrac{1}{24}\Big(-6\alpha\Big(\dfrac{1-m}{1+m}\Big)F(3) - \dfrac{1}{6}c_0 + \dfrac{2m}{3(1+m)}c_0 + \dfrac{1}{3}Dc_0\Big), \\ \Theta(3) = \dfrac{1}{6}\Big(-6\Theta(0)\Theta(3) - (2\epsilon+4)\Theta(1)\Theta(2) + \Big(\dfrac{Pr}{1+R}\Big)(2F(0)\Theta(2) + F(1)\Theta(1))\Big) \\ \qquad = \dfrac{1}{6}\Big(-6\Theta(3) - (\epsilon c_1 + 2c_1)\Theta(2) + \Big(\dfrac{Pr}{1+R}\Big)(2\alpha\Big(\dfrac{1-m}{1+m}\Big)\Theta(2) + 0.25c_1)\Big), \\ \qquad \vdots \end{cases} \tag{32}$$

In the same manner, the rest of components can be obtained using the MATHEMATICA package. Substituted the quantities listed on (32) in (28), when $\eta_0 = 0$, the approximate solution in a series form of the proposed problems (17)−(18) is given by

$$f(\eta) \cong \sum_{k=0}^{n} F(k)\eta^k = F(0) + F(1)\eta + F(2)\eta^2 + F(3)\eta^3 + F(4)\eta^4 + \cdots + F(n)\eta^n, \tag{33}$$

$$\theta(\eta) \cong \sum_{k=0}^{n} \Theta(k)\eta^k = \Theta(0) + \Theta(1)\eta + \Theta(2)\eta^2 + \Theta(3)\eta^3 + \Theta(4)\eta^4 + \cdots + \Theta(n)\eta^n. \tag{34}$$

Now, we find the constants c_0 and c_1 using the boundary conditions (19)−(20), where we take the values $\alpha = 0.2$, $m = 0.5$, $D = 0.5$, $R = 0.5, Pr = 1$, and $\epsilon = 0.2$. These values are $c_0 = 0.143\,818\,606$ and $c_1 = -0.236\,093\,966$. Having $F(k)$, $\Theta(k)$, $k = 0, 1, \cdots, n$, the solution are the same as (33).

5 Results and discussion

Tables 2 and 3 clearly reveal that present solution namely DTM shows excellent agreement with the existing solutions in the literature [16]. This analysis shows that DTM suits for the problems of boundary layer flow in fluid-saturated porous medium. This section provides the behavior of parameters involved in the expressions of heat transfer characteristics for the stretching sheet. Numerical evaluation for the solutions of this problem is performed and the results are illustrated graphically in Figs. 2−10. The study of flow in porous media is very important in approximating the shape of spherical particles or cylindrical fibers which better fit the model of permeability assumed for the analysis. Effects of the porous parameter D on velocity and temperature profiles are shown in Figs. 2 and 3, respectively. It is observed that the velocity decreases for increasing values of porous parameter. Furthermore, the momentum boundary layer thickness decreases as porous parameter D increases. Figure 3 elucidates that the fluid temperature enhances with an increase in the porous parameter.

Table 2 Comparison of numerical value of $-f''(0)$, obtained by DTM for $\alpha = 0.5, D = 0$ with Fang et al.[16]

m	10.00	9.00	7.00	5.00	3.00	2.00	1.00	0.50	0.00	−0.50
$-f''(0)$	1.060 3	1.058 9	1.055 0	1.048 6	1.035 9	1.023 4	1.000 0	0.979 9	0.957 6	1.166 7
Present work	1.061 1	1.058 6	1.054 8	1.048 4	1.035 8	1.023 3	0.998 9	0.979 9	0.957 6	1.166 5

Table 3 Comparison of numerical value of $-f''(0)$, obtained by DTM for $\alpha = 0.25, D = 0$ with Fang et al.[16]

m	10.00	9.00	7.00	5.00	3.00	1.00	0.50	0.00	−1/3	−0.50
$-f''(0)$	1.143 3	1.140 4	1.132 3	1.118 6	1.090 5	1.000 0	0.933 8	0.784 39	0.500 0	0.083 3
Present work	1.143 2	1.141 1	1.132 1	1.118 4	1.090 1	0.997 9	0.933 43	0.784 10	0.499 9	0.083 2

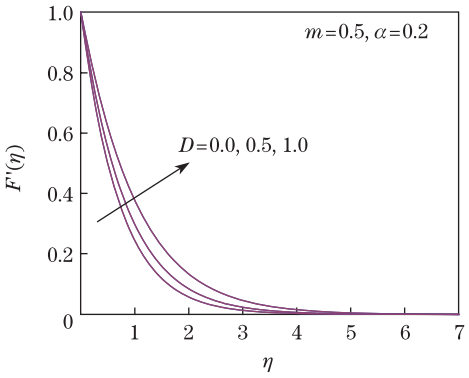

Fig. 2 Behavior of velocity distribution for various values of D

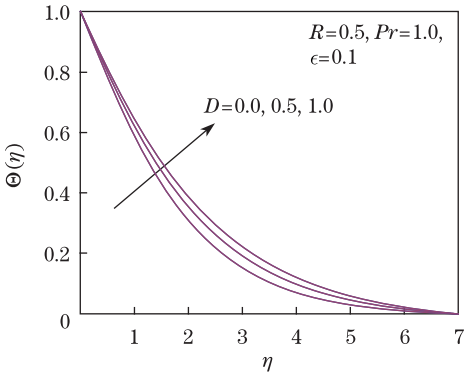

Fig. 3 Behavior of temperature distribution for various values of D

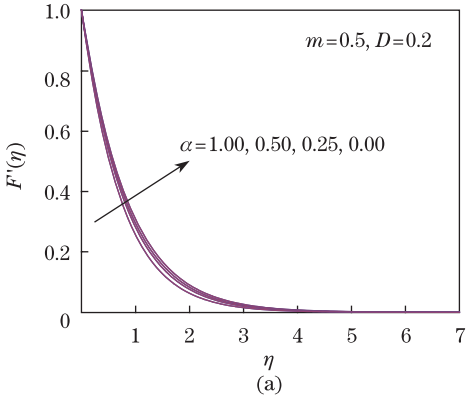

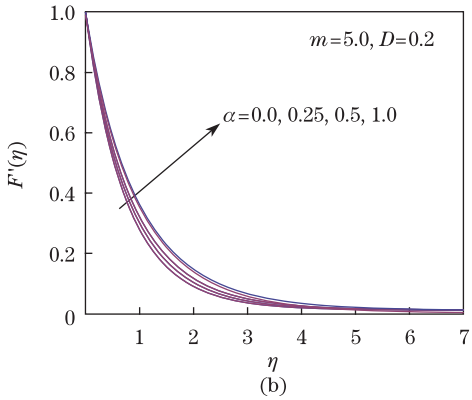

Fig. 4 (a) Behavior of velocity distribution for various values of α with $m = 0.5$ and (b) behavior of velocity distribution for various values of α with $m = 5.0$

The effects of wall thickness parameter on the fluid flow and the temperature distribution have been analyzed and the results are presented in Figs. 4−5. From Fig. 4, it is clear that the

velocity at any point near to the plate decreases as the wall thickness parameter increases for $m < 1$ and the reverse is true for $m > 1$. Also, it is obvious from these figures that the thickness of the boundary layer becomes thinner for a higher value of α when $m < 1$ and becomes thicker for a higher value of α when $m > 1$.

Figure 5 displays that the wall thickness parameter decreases the thickness of the thermal boundary layer and enhances the rate of heat transfer for $m < 1$ whereas reverse trend is observed as $m > 1$. Physically, increasing the value of α when $m < 1$ will decrease the flow velocity, because under the variable wall thickness, not all the pulling force of the stretching sheet can be transmitted to the fluid causing a decrease for both friction between the fluid layers and temperature distribution for the fluid. However, when $m > 1$ the velocity of the flow layers will increase causing an enhance for the friction force between this layers and thus increasing its temperature. Likewise, for a higher value of α, the thermal boundary layer becomes thinner when $m < 1$ compared with the case of $m > 1$.

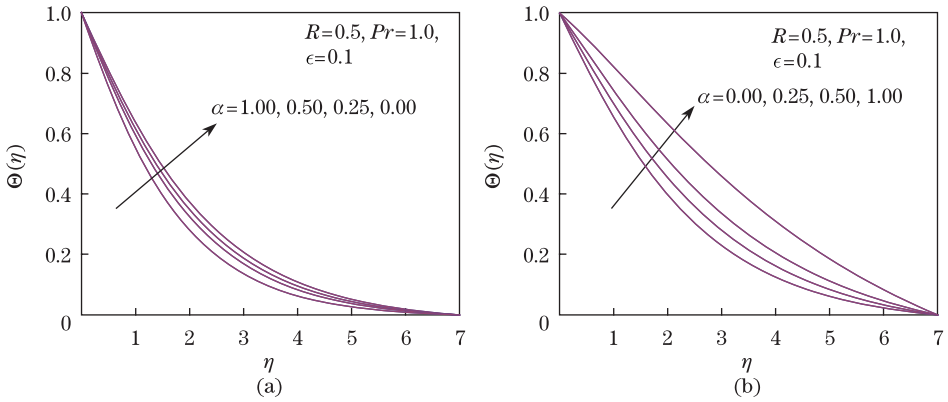

Fig. 5 (a) Behavior of temperature distribution for various values of α with $m = 0.5$ and (b) behavior of temperature distribution for various values of α with $m = 5.0$

Figure 6 shows that the velocity rises with a decrease in the values of the velocity power index m. This implies the momentum boundary thickness becomes thinner as m increases along the sheet, and the reverse is true away from it.

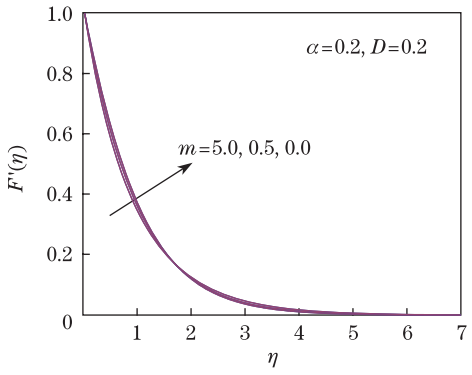

Fig. 6 Behavior of velocity distribution for various values of m

Figure 7 displays the influence of the velocity power index parameter m on the temperature profiles. It is clearly seen from this figure that increasing the value of m produces an increase

in the temperature profiles. It further shows that the larger the value of m, the higher the magnitude of the thermal boundary thickness will be.

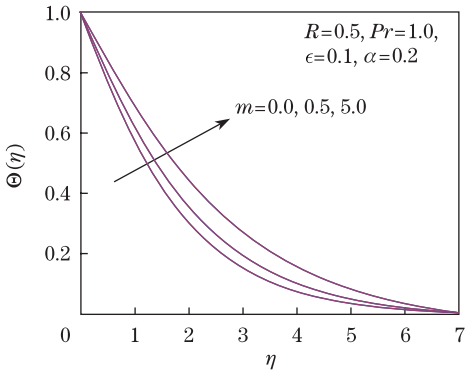

Fig. 7 Behavior of temperature distribution for various values of m

In Fig. 8, we have varied the thermal conductivity parameter ϵ keeping the values of all other parameters fixed. Figure 8 reveals that the temperature profile as well as the thickness of the thermal boundary layer increases when ϵ increases.

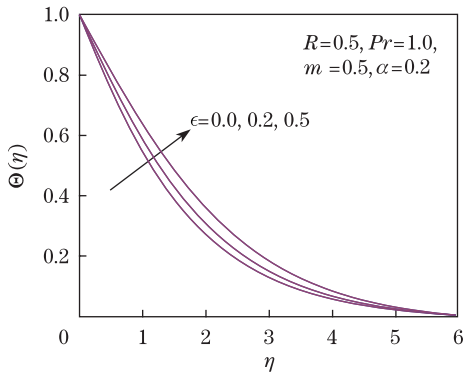

Fig. 8 Behavior of temperature distribution for various values of ϵ

Figure 9 illustrates the effects of radiation parameter R on the temperature profiles when other parameters hold constant. It is depicted that the temperature field and the thermal boundary layer thickness increase with the increase in R.

It is observed from Fig. 10 that an increase in the Prandtl number results in decreasing the heat transfer profiles. The reason is that increasing values of Prandtl number is equivalent to decreasing the thermal conductivities, and therefore heat is able to diffuse away from the heated sheet more rapidly. Hence, in the case of increasing Prandtl number, the boundary layer is thinner and the heat transfer is reduced.

Table 4 shows the influence of the porous parameter D, wall thickness parameter α, the velocity power index parameter m, the radiation parameter R, the Prandtl number Pr, and thermal conductivity parameters ϵ on the local skin friction coefficient and the local Nusselt number. It is noticed that increasing the wall thickness parameter leads to an increase in both the local skin-friction coefficient and the local Nusselt number. Likewise, the local Nusselt number is reduced but the skin-friction coefficient is increased with increasing for both values of porous parameter and velocity power index parameter. Also, an increase in the Prandtl number

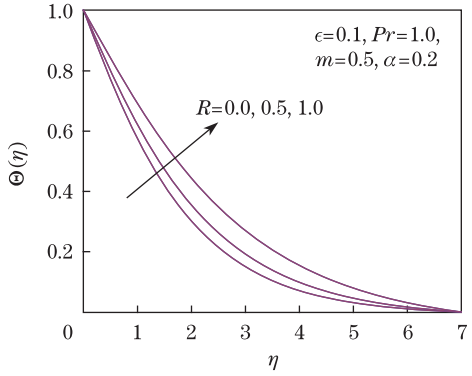

Fig. 9 Behavior of temperature distribution for various values of R

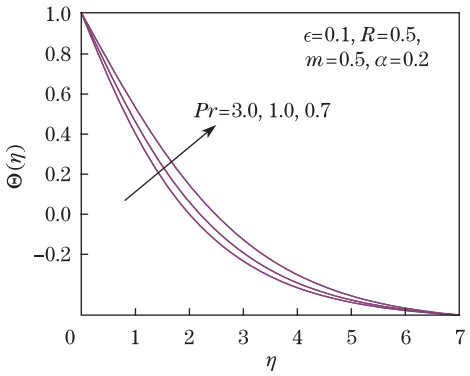

Fig. 10 Behavior of temperature distribution for various values of Pr

causes an increase in the local Nusselt number. This is because a fluid with larger Prandtl number possesses larger heat capacity, and hence intensifies the heat transfer. Moreover, it is observed that the values of the local Nusselt number decrease with increase in both the thermal conductivity parameter and the radiation parameter.

Table 4 Values of $-f''(0)$ and $-\theta'(0)$ for various values of $D, \alpha, m, \epsilon, R$, and Pr

D	α	m	ϵ	R	Pr	$-f''(0)$	$-\theta(0)$
0.0	0.2	0.5	0.1	0.5	1.0	0.924 134	0.441 845 1
0.5	0.2	0.5	0.1	0.5	1.0	1.168 475	0.401 814 8
1.0	0.2	0.5	0.1	0.5	1.0	1.369 671	0.372 276 5
0.5	0.0	0.5	0.1	0.5	1.0	1.133 980	0.375 123 1
0.5	0.25	0.5	0.1	0.5	1.0	1.177 211	0.408 650 4
0.5	0.5	0.5	0.1	0.5	1.0	1.222 213	0.443 231 2
0.5	1.0	0.5	0.1	0.5	1.0	1.316 454	0.515 111 9
0.5	0.2	0.0	0.1	0.5	1.0	1.044 345	0.472 759 0
0.5	0.2	0.5	0.1	0.5	1.0	1.168 209	0.401 889 7
0.5	0.2	5.0	0.1	0.5	1.0	1.327 408	0.303 387 3
0.5	0.2	0.5	0.0	0.5	1.0	1.168 209	0.434 831 0
0.5	0.2	0.5	0.2	0.5	1.0	1.168 209	0.373 923 1
0.5	0.2	0.5	0.5	0.5	1.0	1.168 209	0.310 607 6
0.5	0.2	0.5	0.1	0.0	1.0	1.168 209	0.547 710 4
0.5	0.2	0.5	0.1	0.5	1.0	1.168 209	0.401 856 9
0.5	0.2	0.5	0.1	1.0	1.0	1.168 209	0.319 519 0
0.5	0.2	0.5	0.1	0.5	0.7	1.168 209	0.302 223 4
0.5	0.2	0.5	0.1	0.5	1.0	1.168 209	0.401 843 5
0.5	0.2	0.5	0.1	0.5	3.0	1.168 209	0.896 387 6

6 Conclusions

Here, we use the DTM to solve the resulting non-linear system of ordinary differential equations (ODEs) of the problem of flow and heat transfer in a quiescent Newtonian fluid flow caused solely by a stretching sheet, which embedded in a porous medium with variable thickness, variable thermal conductivity, and thermal radiation. The fluid thermal conductivity is assumed to vary as a linear function of temperature. Comparison with previously published work is performed and the results are found to be in excellent agreement. Asystematic study on the effects of the various parameters on flow and heat transfer characteristics is carried out. It is found that increasing values of the porous parameter, the velocity power index parameter, thermal conductivity parameter, and the radiation parameter reduces the local Nusselt number.

On the other hand, it is observed that the local Nusselt number increases as the Prandtl number and the wall thickness parameter increase. Moreover, it is interesting to find that increasing the porous parameter, wall thickness parameter, and the velocity power index parameter in magnitude, causes the fluid to slow down past the stretching sheet and the increasing of skin-friction coefficient in magnitude. Summarizing these results, we can say that the DTM in its general form gives a reasonable calculation, easy to use, and can be applied for the differential equations in general form.

References

[1] Crane, L. J. Flow past a stretching plate. *Zeitschrift für angewandte Mathematik und Physik*, **21**, 645–647 (1970)

[2] Gupta, P. S. and Gupta, A. S. Heat and mass transfer on a stretching sheet with suction or blowing. *The Canadian Journal of Chemical Engineering*, **55**(6), 744–746 (1979)

[3] Soundalgekar, V. M. and Ramana, T. V. Heat transfer past a continuous moving plate with variable temperature. *Wärme-und Stöffübertrag-ung*, **14**, 91–93 (1980)

[4] Grubka, L. J. and Bobba, K. M. Heat transfer characteristics of a continuous stretching surface with variable temperature. *Heat and Mass Transfer*, **107**, 248–250 (1985)

[5] Chen, C. K. and Char, M. Heat transfer on a continuous stretching surface with suction or blowing. *Journal of Mathematical Analysis and Applications*, **35**, 568–580 (1988)

[6] Hayat, T., Abbas, Z., and Javed, T. Mixed convection flow of a micropolar fluid over a non-linearly stretching sheet. *Physics Letters A*, **372**, 637–647 (2008)

[7] Cheng, P. and Minkowycz, W. J. Free convection about a vertical flat plate embedded in a porous medium with application to heat transfer from a dike. *Journal of Geophysical Research: Atmospheres*, **82**, 2040–2044 (1977)

[8] Elbashbeshy, E. M. A. and Bazid, M. A. A. Heat transfer in a porous medium over a stretching surface with internal heat generation and suction or injection. *Applied Mathematics and Computation*, **158**, 799–807 (2004)

[9] Cortell, R. Flow and heat transfer of a fluid through a porous medium over a stretching surface with internal heat generation/absorption and suction/blowing. *Fluid Dynamics Research*, **37**, 231–245 (2005)

[10] Hayat, T., Abbas, Z., Pop, I., and Asghar, S. Effects of radiation and magnetic field on the mixed convection stagnation-point flow over a vertical stretching sheet in a porous medium. *International Journal of Heat and Mass Transfer*, **53**, 466–474 (2010)

[11] Hossain, M. A., Alim, M. A., and Rees, D. The effect of radiation on free convection from a porous vertical plate. *International Journal of Heat and Mass Transfer*, **42**, 181–191 (1999)

[12] Hossain, M. A., Khanfer, K., and Vafai, K. The effect of radiation on free convection flow of fluid with variable viscosity from a porous vertical plate. *International Journal of Thermal Sciences*, **40**, 115–124 (2001)

[13] Elbashbeshy, E. M. A. and Dimian, M. F. Effects of radiation on the flow and heat transfer over a wedge with variable viscosity. *Applied Mathematics and Computation*, **132**, 445–454 (2002)

[14] Abel, M. S. and Mahesha, N. Heat transfer in MHD viscoelastic fluid flow over a stretching sheet with variable thermal conductivity, non-uniform heat source and radiation. *Applied Mathematical Modelling*, **32**, 1965–1983 (2008)

[15] Bataller, R. C. Radiation effects in the Blasius flow. *Applied Mathematics and Computation*, **198**, 333–338 (2008)

[16] Fang, T., Zhang, J., and Zhong, Y. Boundary layer flow over a stretching sheet with variable thickness. *Applied Mathematics and Computation*, **218**, 7241–7252 (2012)

[17] Khader, M. M. On the numerical solutions for the fractional diffusion equation. *Communications in Nonlinear Science and Numerical Simulation*, **16**, 2535–2542 (2011)

[18] Khader, M. M. and Megahed, A. M. Numerical simulation using the finite difference method for the flow and heat transfer in a thin liquid film over an unsteady stretching sheet in a saturated

porous medium in the presence of thermal radiation. *Journal of King Saud University Engineering Sciences*, **25**, 29–34 (2013)

[19] Khader, M. M., Talaat, S. D., and Hendy, A. S. A computational matrix method for solving systems of high order fractional differential equations. *Applied Mathematical Modelling*, **37**, 4035–4050 (2013)

[20] Sweilam, N. H., Khader, M. M., and Adel, M. Numerical simulation of fractional Cable equation of spiny neuronal dendrites. *Journal of Advanced Research,* **1**(1), 59–67 (2013)

[21] Sweilam, N. H., Khader, M. M., and Nagy, A. M. Numerical solution of two-sided space fractional wave equation using finite difference method. *Computational and Applied Mathematics*, **235**, 2832–2841 (2011)

[22] Khader, M. M., Sweilam, N. H., and Mahdy, A. M. S. Numerical study for the fractional differential equations generated by optimization problem using Chebyshev collocation method and FDM. *Applied Mathematics Information Science*, **7**(5), 2011–2018 (2013)

[23] Zhou, J. K. *Differential Transformation and Its Application for Electrical Circuits*, Huazhong University Press, Wuhan (1986)

[24] Borhanifar, A. and Abazari, R. Numerical study of nonlinear Schrödinger and coupled Schrödinger equations by differential transformation method. *Optics Communications*, **283**, 2026–2031 (2010)

[25] Abazari, R. and Borhanifar, A. Numerical study of the solution of the Burger and coupled Burger's equations by a differential transformation method. *Computers and Mathematics with Applications*, **59**, 2711–2722 (2010)

[26] Bildik, N. and Konuralp, A. The use of variational iteration method, differential transform method and Adomian decomposition method for solving different type of nonlinear partial differential equations. *International Journal of Nonlinear Scince and Numerical Simulation*, **7**(1), 65–70 (2006)

[27] Jang, M. J., Chen, C. L., and Liy, Y. C. Two-dimensional differential transform for partial differential equations. *Applied Mathematics and Computation*, **121**, 261–270 (2001)

[28] Ozdemir, O. and Kaya, M. O. Flapwise bending vibration analysis of a rotating tapered cantilever Bernoulli-Euler beam by differential transform method. *Journal of Sound and Vibration*, **289**, 413–420 (2006)

[29] Arikoglu, A. and Ozkol, I. Solutions of integral and integro-differential equation systems by using differential transform method. *Computers and Mathematics with Applications*, **56**, 2411–2417 (2008)

[30] Arikoglu, A. and Ozkol, I. Solution of difference equations by using differential transform method. *Applied Mathematics and Computation*, **174**, 1216–1228 (2006)

[31] Raptis, A. Flow of a micropolar fluid past a continuously moving plate by the presence of radiation. *International Journal of Heat and Mass Transfer*, **41**, 2865–2866 (1998)

[32] Raptis, A. Radiation and viscoelastic flow. *International Communications in Heat and Mass Transfer*, **26**, 889–895 (1999)

[33] Chiam, T. C. Magnetohydrodynamic heat transfer over a non-isothermal stretching sheet. *Acta Mechanica*, **122**, 169–179 (1997)

[34] Mahmoud, M. A. A. and Megahed, A. M. MHD flow and heat transfer in a non-Newtonian liquid film over an unsteady stretching sheet with variable fluid properties. *Canadian Journal of Physics*, **87**, 1065–1071 (2009)